Mechanics of Advanced Composite Structures

Journal homepage: https://macs.semnan.ac.ir/

Semnan University

ISSN: 2423-7043

Research Article

Influence of Process Parameters on the Mechanical Properties of Carbon Fibre Reinforced PETG

Prabhakaran Ramachandran [a]*, Pitchipoo Pandian [b], Venkatesh Ramamoorthi [a], Jerold John Britto John [a]

[a] *Department of Mechanical Engineering, Ramco Institute of Technology, Rajapalayam, 626 117, Tamil Nadu, India*

[b] *Department of Mechanical Engineering, P.S.R. Engineering College, Sivakasi, 626140, Tamilnadu, India*

ARTICLE INFO

Article history:

Received: 2025-01-08

Revised: 2025-06-30

Accepted: 2025-07-14

Keywords:

Carbon fibre;

Polyethylene Terephthalate Glycol (PETG);

Mechanical properties;

Thermal properties;

Fused Filament Fabrication (FFF).

ABSTRACT

The research analyses the impact of different compositions of carbon fibre on mechanical and thermal attributes of Fused Filament Fabricated (FFF) Polyethylene Terephthalate Glycol (PETG) composites. Three different types of carbon fibre composite (10%, 20%, and 30% content) were manufactured for analysis against pure PETG material. The tests analysed the mechanical performance through compressive strength analysis, along with flexural strength measurements and measurements of hardness. The characterizing tests included Vicat Softening Temperature alongside Heat Deflection Temperature assessment. The research used ASTM standard testing methods to validate experimental measurements through finite element simulations using ANSYS Workbench ACP®. Integration of carbon fibre components improved the total mechanical behaviour of the PETG material. PETG without fibre demonstrated 53 MPa compressive strength, while 30% CF-PETG achieved 58 MPa compressive strength. The flexural strength measurements mirrored those changes, starting from 54 MPa and reaching 80 MPa across the same compositions. The Shore Hardness measurement (D) experienced an elevation as the carbon fibre concentration in materials grew from 71 to 77. Vicat Softening Temperature and Heat Deflection Temperature values improved alongside carbon fibre content increases. The experimental results matched closely with simulation outputs from the analysis, thus validating its accuracy. Research data shows that PETG materials improve their mechanical and thermal qualities when carbon fibre is incorporated, thereby creating promising prospects for specific applications needing advanced performance levels.

1. Introduction

Additive manufacturing has emerged versatile technology aimed at producing precisely shaped components. 3D printing has transformed the production system by offering significant flexibility in custom manufacture, high precision, and the capacity to provide composite materials [1]. Fused filament (FFF) fabrication method is a widespread additive manufacturing technique that facilitates a simple, additional, versatile, and cost-effective method for producing purposeful products. But a significant limitation of additive manufacturing processing is inadequate dimensional and geometric performance, which restricts the production of higher-quality effective components [2]. Newly, in the aviation and

* **Corresponding author.**
E-mail address: *prabhakaranrresearch@gmail.com*

Cite this article as:

Ramachandran, P., Pandian, P., Ramamoorthi, V. and John, J.J.B., 2026. Influence of Process Parameters on the Mechanical Properties of Carbon Fibre Reinforced PETG. *Mechanics of Advanced Composite Structures*, 13(1), pp. 171-184.

https://doi.org/10.22075/MACS.2025.36494.1791

automotive industries, using fused deposition modeling (FDM), polyethylene terephthalate (PETG) glycols, and carbon fibre-strengthened polyethylene terephthalate glycols (CF-PETG) composites have emerged as exceptional material alternatives. In the system of FDM, the process parameters distress the dimensional stability, consistency, and characteristics of the printed varieties [3]. Carbon fibres (CFs) act as reinforcement in the fabrication of a PETG-based composite with the FDM printing method. The impact of CF and process variables on infill pattern and percentage, with its layer thickness, was examined by assessing the tensile, flexural, and compressive characteristics of the produced polymer composite material [4]. The composite is made using 33.34% PLA printed primarily, succeeded in 33.33% PETG, and ultimately 33.33% ABS, resulting in PETG being interposed between ABS and PLA. The influence of FFF processing settings on the tensile characteristics of the printed composites was examined [5]. The mechanical properties of CF/PETG materials have been evaluated using a model that was quantitatively correlated with the experimental findings. Scanning electron microscopy was employed to assess the fracture surface [6]. In the domain of damage finding in carbon fibre reinforced (CFRP) plastics, fibre optic sensors (FOS) are crucial due to their beneficial characteristics, including low weight, cost-effectiveness, broad availability, corrosion resistance, and immunity to electromagnetic interference. A significant amount of advanced research on the detection of CFRP damage utilises different fibre optic sensors, including fibre Bragg (FBG) grating [7]. Carbon fibre strengthened dual-matrix composites (CHM) exhibit significant promise in the domain of artificial bone applications owing to their low density, high specific strength, and superior biocompatibility[8].

Additive manufacturing materials can be evaluated using tensile testing, Charpy/Izod impact tests, shearing, and bending etc. Izod is the most common way to test the impact strength of plastics [9]. Examine the dynamic strength of PETG thermoplastics strengthened with carbon fibre and optimise the different process settings. Nine sets of tensile and flexural specimens are manufactured according to ASTM standards [10]. The incorporation of carbon fibre into PETG polymers adversely impacted flatness, dimensional accuracy, and surface roughness across most printing circumstances, markedly diminishing the combinations of printing parameters that yielded ideal values [11]. PETG has become a suitable biomaterial for several medical applications, including dentistry, orthopaedics, cardiology, neurology, and surgery. PETG plays a significant role in biological research and engineering by enhancing cell studies, drug delivery systems, and antibacterial applications [12]. In tensile evaluation, the short-length fibre material exhibited a comparable trend to various compressive tests, demonstrating enhanced strength at elevated rates of strain. This occurred because of the elevated strain rate, which led to a more rapid fracture, hence diminishing the time available for matrix cracking prior to final failure by fibre pull-out [13]. The stress relaxing behaviour indicated a reduction in compressive stresses with time for pure PETG, but the creep response facilitated increased compressive displacements [14]. The contraction of PETG printed specimens transpired in the printing direction as the temperature approached the transition point. Modifying the printing settings and shape can provide many applications, and its integration with the novel biocompatible material may prove to be more exciting [15]. The innovative cellular coil employed in experiments originated under the idea that decreasing the distance between heating regions may mitigate problems related to the inadequate in-plane thermal conductivity observed in CFRP composites [16]. In terms of longitudinal strength and modulus, PA-CF showed more predictability compared to PLA-CF, ABS-CF, and PETG-CF, whereas PLA-CF and ABS-CF exhibited higher predictability regarding transverse modulus. Fractography revealed that fibre orientation, porosity, fibre length, and poor matrix-fibre interfacial bonding are the primary sources of prediction error [17].

Investigated how different FDM process factors, notably layer thickness, raster angle, and print speed, influence the mechanical characteristics of 3D print PETG specimens reinforced with carbon fibre (CF). Optimal parameters, including a 0° raster angle, a layer thickness is 0.2 mm, and a 40 mm/s print speed, expand both flexural and tensile strength by enhancing material bonding and alignment [18]. The novel of printed 3D hybrid continuous fibre reinforced bi-matrix composites aimed at enhancing fracture flexural energy and design ability for flexural mechanical attributes. It combines the superior wettability of thermosetting resins with various fibres and the exceptional extrusion forming capability of thermoplastic for the nozzle-based method of additive manufacturing [19]. Innovations in three-dimensional printing utilising plastic waste, notably concentrating on fused deposition modeling and selective laser sintering techniques for carbon fibre composites. The significance of materials in the process of 3D printing, particularly with the

challenges associated with the production of non-recyclable polymers [20]. Digital light processing (DLP) printed test products were fabricated with an ultraviolet-sensitive resin, as the study concentrated on assessing the effects of surface quality and durability, in accordance with ASTM criteria. Taguchi and Grey relational optimisation approaches were utilised to enhance the DLP printing process by identifying optimal values for various parameters [21]. Components for three-point bending, constructed from continuous carbon fibre reinforced PLA, were produced by 3D printing and then underwent three-point bending compression fatigue testing. The coupons were initially exposed to 105 cycles under varying loads, after which a three-point bending test [22] was performed. The machining of the factory-produced PLA and PETG coupons was experimentally examined using a standard dry turning technique. Mechanical factors, including hardness and roughness, may be assessed both before and after the machining processes [23]. To conduct different testing on 3D printed objects, choosing the optimal printing process parameters is crucial. Impact, tensile, and hardness tests were conducted to determine the optimal parameters for achieving superior mechanical characteristics [24]. The source of digital projection light is employed to solidify the surfaces of liquid photopolymer in the DLP method. This method is optimal for objects with intricate geometries and minimal cross-sectional dimensions that require superior surface quality and strength of the object [25].

The study investigates PETG composites reinforced with 10%, 20% and 30% carbon fiber through FFF 3D printing. The research validity is guaranteed by experimental results as well as FESEM analysis. Researchers have identified 30% CF-PETG as a breakthrough material for aerospace and automotive industries since it combines excellent stiffness-to-weight performance with enhanced damping characteristics.

2. Materials and Methods

2.1. 3D Printing Machine and Materials

One of the most popular technologies in the world today is 3D printing, which allows for the creation of complex shapes with the least amount of material wasted, and the creation of ASTM-standard shapes for compressive, flexural, hardness and heat deflection and softening temperature specimens using a URU 3.0 FDM 3D printer (without enclosure). A 3D printer with a build volume of 220 x 220 x 250 mm was utilised for this investigation. Its maximum extruder temperature is 320 degrees Celsius, and its maximum bed temperature is 100 degrees Celsius. Additional printer specifications are provided in Table 1, and Figure 1 displays an image of the 3D printer.

In this study, chopped carbon reinforced with PETG filament is employed as a 3D printing material, with 10%, 20%, and 30% carbon combined with the corresponding 90%, 80%, and 70% PETG materials, as mentioned in Figure 2. This work mainly focuses on investigating the mechanical characteristics of carbon reinforced PETG material, comparing the 10% CF-PETG, 20% CF-PETG, and 30% CF-PETG findings to the pure PETG material, and verifying the results using numerical simulation results. The ASTM standard material was modeled using Creo Parametric 9.0®, with numerical analysis performed using Ansys Workbench 23.0®.

M/s.Medsby Health Care Solutions and Flash-Forge from India manufactured customized filament with density 1.27-1.38 g/cm3, water absorption 0.2-0.5% (24Hr), Glass Transition Temperature (Tg) 75–85°C, Melting Temperature 230–260°C, Heat Deflection Temperature (HDT) 60–70°C (at 0.45 MPa), Flexural Strength 75–100 MPa, Impact Strength (Izod, Notched) 3.0–8.0 kJ/m^2, Hardness (Shore D) 76–80, Coefficient of Thermal Expansion (CTE) ~50–70 µm/m°C and FDM 3D printer used for the test coupon fabrication; the printer specifications are listed in Table 2. Cura software is used for slicing and generating the G codes of the test coupons, Creo Parametric 9.0® modeling software is used to prepare the solid model, and the ANSYS 23® ACP module is used to simulate the model in accordance with the ASTM standard. M/s.Medsby Health Care Solutions and Flash-Forge prepared filament by incorporating carbon fibre into PETG at different weight percentages (10%, 20%, and 30%). The mixing process was carried out through a twin-screw extruder to ensure the homogeneous distribution of carbon fibres inside the PETG matrix. The extruded filament was subsequently chilled and spooled to be used later for utilisation in MEX 3D printing. The mechanical properties of the filaments were evaluated to ensure uniformity across various compositions. This composite material was utilised in MEX 3D printing to evaluate its potential for high-strength, lightweight applications, in engineering and industrial components requiring improved mechanical performance. The choice of PETG as the material of base was based on its exceptional thermal stability, printability, and impact resistance, making it the best alternative for reinforcing with carbon

fibres. The study intended to examine the impact of carbon fibre incorporation on the structural integrity and mechanical properties of PETG composites, confirming their applicability for practical uses.

The different filament manufacturer brands of filament were used in the Flash Forge 3D printer to produce test coupons in all CFRP-PETG combinations according to the ASTM specifications. To check Geometric Dimensioning Tolerances (GD&T) and allowances, all test coupons were pre-checked using a Coordinate Measuring Machine (CMM) to ensure their dimensional stability.

Table 1. FDM 3D Printer

Model	Specifications
Build Volume	220×220×250 mm
No of Extruders	1
Resolution	100 – 300 microns
Supporting Materials	PLA, PETG, CF-PETG, TPU, ABS & PVC
File Format	.stl & gcode
Material diameter	1.75 mm
Host computer Software	Repetier-Host Cura

Fig. 1. URU 3.0 FDM 3D Printer

Fig. 2.a. Pure PETG Filament

Fig. 2.b. 10% CF-PETG Filament

Fig. 2.c. 20% CF-PETG Filament

Fig. 2.d. 30% CF-PETG Filament

Fig. 2. PETG Filaments

2.2. Printing Procedure and Parameters

The majority of the literature suggests that using a 100% infill density in 3D printing materials results in superior mechanical properties. The ASTM standard components mentioned in Figure 4 used in this study were manufactured using the FDM 3D printer. The 3D printing software was configured with appropriate parameters to ensure efficient printing of the components. The printer was set to a nozzle temperature of 240 degrees Celsius and a bed temperature of 85 degrees Celsius. The nozzle diameter used for this study was 0.4 mm. The test samples were printed with a layer height of 0.1 mm. The specifications for the printing parameters and the procedures are provided in Table 2 and a corresponding Figure 3.

Table 2. Printing Parameters

Name	Range
Material	PETG + (10%, 20% & 30% carbon fibre)
Printing speed	80 mm/sec
Infill density	100%
Raster angle	45°C / -45 °C
Printing pattern	Line pattern
Nozzle temperature	170°C – 320°C
Platform temperature	85 °C
Layer thickness	0.1 mm

In the 3D printing process, the first step involved obtaining the ASTM standard part file, which was designed using the Creo Parametric 9.0® software. The solid file was then imported into the slicing software, where the dimensions and starting point for the printer were determined. The printer is capable of printing PETG, 10% CF-PETG, 20% CF-PETG, and 30% CF-PETG filaments. The printing parameters were set using the control screen on the printer. During the printing process, the filament was heated to 240°C in the extrusion chamber and then flowed through the nozzle. The nozzle

moves according to the desired pattern, resulting in the printing of the part on the bed. Once the printing process was completed, the finished part was separated from the bed.

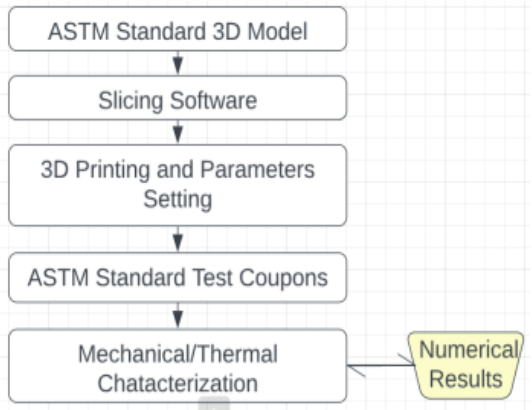

Fig. 3. Step by Step Procedure - Flow Chart

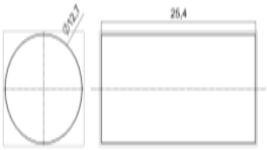

Fig. 4a. ASTM D695 for Compression Test

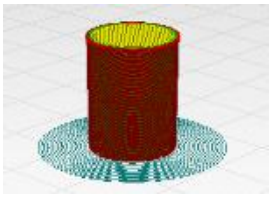

Fig. 4b. ASTM D695 - Slicing Software Model

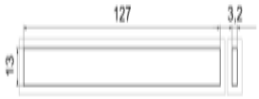

Fig. 4c. ASTM D790 for Flexural Test

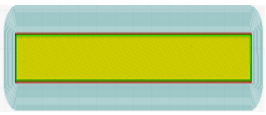

Fig. 4d. ASTM D790 - Slicing Software Model

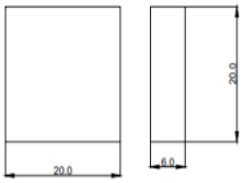

Fig. 4e. ASTM E384 for Shore Hardness Test D

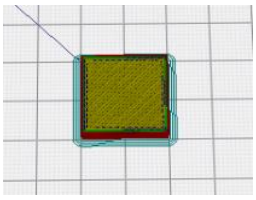

Fig. 4f. ASTM E384 - Slicing Software Model

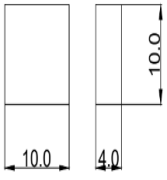

Fig. 4g. ASTM D1525 for Vicat Softening Temperature

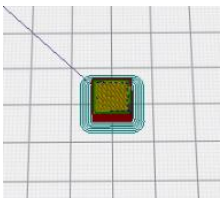

Fig. 4h. ASTM D1525 - Slicing Software Model

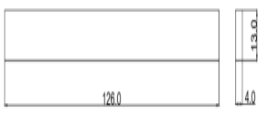

Fig. 4i. ASTM D648 for Heat Deflection Temperature

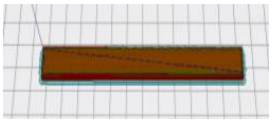

Fig. 4j. ASTM D648 - Slicing Software Model

Fig. 4. Dimensions of ASTM Standard Specimens

3. Experimental Work

3.1. Compression Test

A schematic diagram of Figure 5 shows the compression test experimental setup. The compression test was performed, and the maximum compression strength of the component is presented in Table 3.

Five specimens were prepared for each composition: PETG, 10% CF-PETG, 20% CF-PETG, and 30% CF-PETG, shown in Figure 6, following the ASTM standard D695. The specimens were created using the FDM 3D printer with a layer height of 0.1 mm and 100% infill density. In the compression test, the material was subjected to a fixed strain rate, and the manufactured component was tested in the Tensile Strength Tester – 10KN by controlling the degree of freedom or motion.

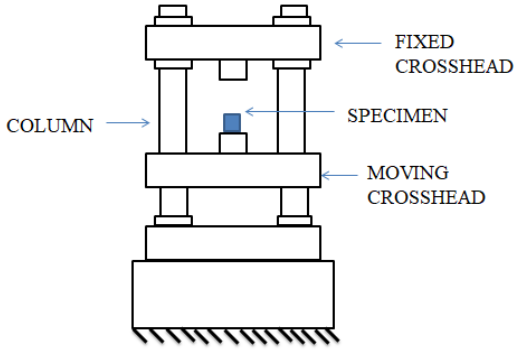

Fig. 5. 2D-Schematic Diagram of Compression Test Experimental Setup

Fig. 6a. Compression Specimen of Pure PETG

Fig. 6b. Compression Specimen of 10% CFPETG

Fig. 6c. Compression Specimen of 20% CF-PETG

Fig. 6d. Compression Specimen of 30% CF-PETG

Fig.6. Compression Test Specimens

Table 3. Experimental results of Compression Test

Material Name	Compressive Strength (MPa)
PETG	53
10% CF-PETG	49
20% CF-PETG	54
30% CF-PETG	58

In the compression test, the chopped carbon fibre was pulled out from the matrix composites. The load-displacement curve demonstrates the relationship between strain rate and stress until the stress reaches the yield point. Prior to the yield point, the material displays elastic properties, while above the yield point and it undergoes plastic deformation. Figures 7, 8, and 9 depict a visual comparison of the values derived from the experimental data.

The marginal reduction in compressive and flexural strength noted in 10% CF-PETG relative to pure PETG can be attributed to the irregular distribution of carbon fibres and possible void development during the extrusion process. While carbon fibres often improve mechanical qualities, at lower concentrations, they may fail to establish a cohesive reinforcement within the polymer matrix. This may result in stress concentration areas and microstructural irregularities, thereby decreasing compressive strength. The incorporation of chopped carbon fibres may interfere with the uniform load distribution in the PETG matrix, resulting in reduced interfacial bonding and increased risk of failure under compressive loads. As the carbon fibre concentration exceeds 10%, the reinforcement effect increases, leading to enhanced compressive strength, as demonstrated in the 20% and 30% CF-PETG samples.

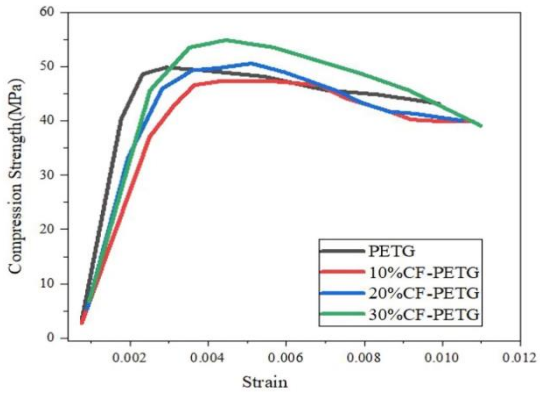

Fig. 7. Strain Curve for Compression Test

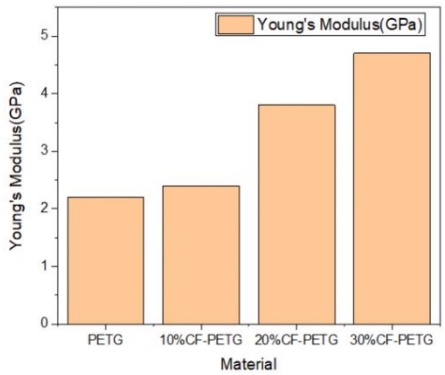

Fig. 8. Young's Modulus of PETG

The compressive forces in Figure 9 were shown as mean values with error bars to show how they varied across different specimens. These differences happen because of small changes in how the material is deposited, how the fibres are aligned, and how the layers stick to each other during the 3D printing process. In Figure 8, on the other hand, Young's modulus was found by looking at the stress-strain curve, which showed values that were mostly the same for all test cases. The modulus of a material changes depending on the starting range of elastic deformation, so there were not many differences in it.

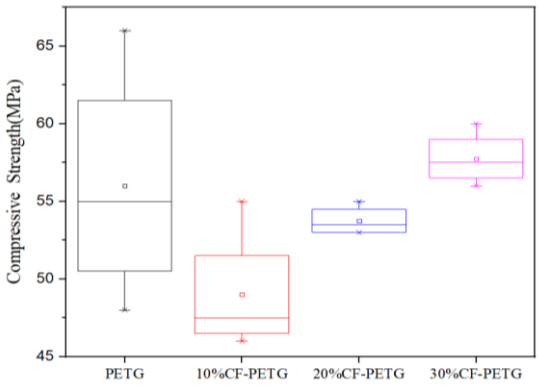

Fig. 9. Comparison of Compressive Strength of PETG

3.2. Flexural Test

The fabricated component undergoes testing with the Tensile Strength Tester – 10KN schematic diagram shown in Figure 10. To conduct a three-point flexural strength test on the 3D printed specimen, the machine holders were modified accordingly.

A total of five samples were created for each composition of PETG, 10% CF-PETG, 20% CF-PETG, and 30% CF-PETG, shown in Figure 11, in accordance with the ASTM standard D790 for conducting flexural strength tests. The specimens were produced via the FDM 3D printer, which does not have an enclosure. The printing process involved employing a layer height of 0.1 mm and a 100% infill density. During the flexural test, the centre point experiences compression, while the lower region undergoes elongation. An important limitation of this test is the measurement of strain during the test.

The resultant number represents the highest bending strength of the component, which is presented in Table 4. Figures 12 and 13 depict a visual comparison of the values derived from the experimental data.

Multiple variables describe how compressive strength ratings do not increase linearly with fibre content. Stress concentrations and irregular load transfer can result from non-

uniform dispersion and agglomeration at greater fibre concentrations. Nonlinear compressive strength trends are also caused by FFF 3D printing voids, fiber-matrix adhesion heterogeneity, and anisotropic fiber orientation. Fibre buckling or debonding replaces matrix yielding as fibre content increases, reducing strength. Future research will optimise printing settings and fibre orientation to increase CF-PETG composite compressive strength consistency.

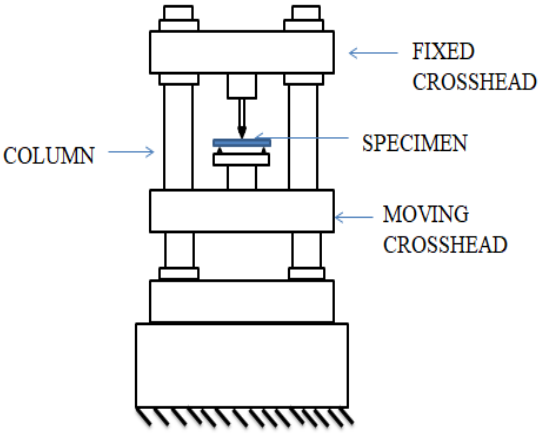

Fig. 10. UTM Machine with Flexural Specimen

Fig. 11a. Flexural Specimen of Pure PETG

Fig. 11b. Flexural Specimen of 10% CF-PETG

Fig. 11c. Flexural Specimen of 20% CF-PETG

Fig. 11d. Flexural Specimen of 30% CF-PETG

Fig. 11. Flexural Specimens

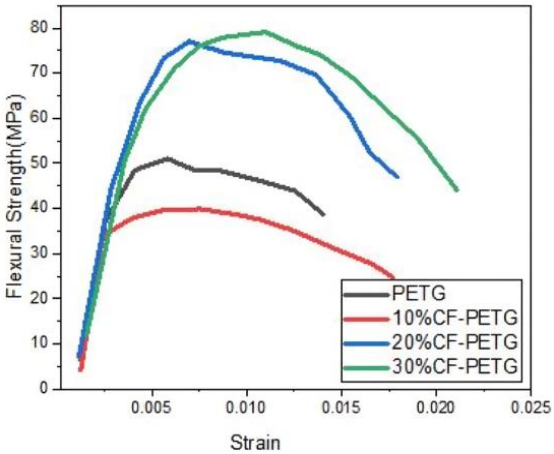

Fig. 12. Stress-Strain Curve for Flexural Test

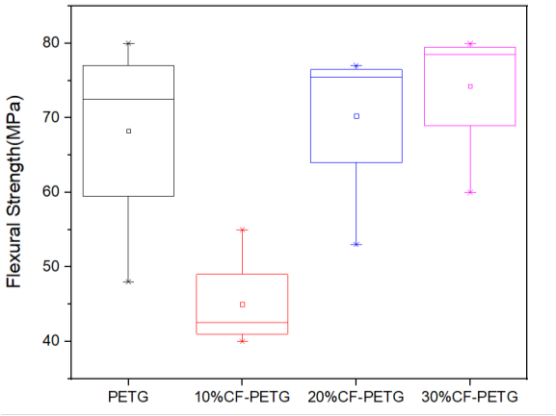

Fig. 13. Comparison of Flexural Strength of PETG

Table 4. Experimental results of the Flexural test and Modulus

Material Name	Flexural Strength (MPa)	Flexural Modulus (GPa)
PETG	54	2.76
10%CF-PETG	43	5.15
20%CF-PETG	77	6.67
30%CF-PETG	80	7.01

3.3. Hardness Test

Five specimens of each composition, PETG, 10% CF-PETG, 20% CF-PETG, and 30% CF-PETG, were prepared according to ASTM standard E384 for the Shore Hardness test D shown in Figure 14 and 15. The specimens were printed using the FDM 3D printer with a layer height of 0.1 mm and 100% infill density.

In this Shore Hardness test, D mentioned a schematic diagram, where the ability to resist scratches was determined through a hardness test. The hardness of the specimens, based on the carbon percentage, is shown in Table 5. Figures 16 depict a visual comparison of the values derived from the experimental data.

The discrepancies in Shore Hardness (D) values across various CF-PETG preparations can be attributed to the increased proportion of carbon fibre reinforcement. As the carbon fibre concentration rises from 10% to 30%, the material's hardness correspondingly increases due to the rigid characteristics of carbon fibres, which enhance overall stiffness and resistance to surface deformation. The recorded Shore Hardness values were 71 for pure PETG, 72 for 10% CF-PETG, 74 for 20% CF-PETG, and 77 for 30% CF-PETG. The enhancement in hardness positively influences mechanical performance by increasing wear resistance and weakening

surface deformation under load. However, elevated hardness may result in enhanced brittleness, thus reducing the material's impact resistance. The equilibrium between hardness and toughness is essential in choosing a suitable CF-PETG formulation for certain applications.

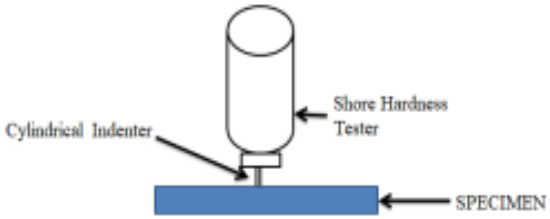

Fig. 14. Schematic Diagram of Shore Hardness Test D

Fig. 15a. Shore Hardness Specimen of pure PETG

Fig. 15b. Shore Hardness Specimen of 10% CF-PETG

Fig. 15c. Shore Hardness Specimen of 20% CF-PETG

Fig. 15d. Shore Hardness Specimen of 30% CFPETG

Fig. 15. Shore Hardness Specimens

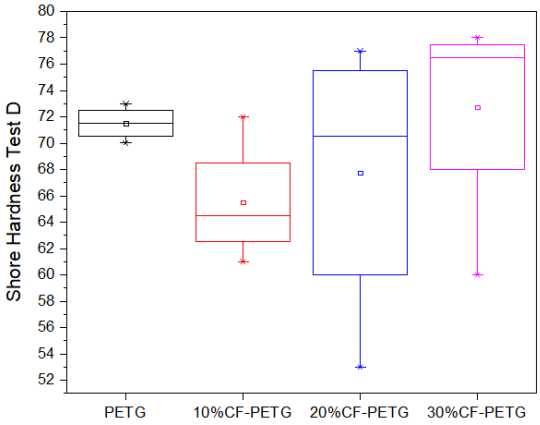

Fig. 16. Comparison of Shore Hardness Test D of PETG

Table 5. Experimental results of the Flexural test

Material Name	Shore Hardness Test D
PETG	71
10%CF-PETG	72
20%CF-PETG	74
30%CF-PETG	77

3.4. Vicat Softening Temperature

The Vicat Softening Temperature was determined by measuring the temperature at which a needle penetrated the specimen in a constant temperature atmosphere, schematic diagram in Figure 17.

Five specimens were prepared for each composition of PETG, 10% CF-PETG, 20% CF-PETG, and 30% CF-PETG, as shown in Figure 18, following the ASTM standard D1525 for the Vicat Softening Temperature test. The specimens were created using the FDM 3D printer with a layer height of 0.1 mm and 100% infill density.

The results for the Vicat Softening Temperature of each specimen, based on the carbon percentage, are presented in Table 6. Figures 19 depict a visual comparison of the values derived from the experimental data.

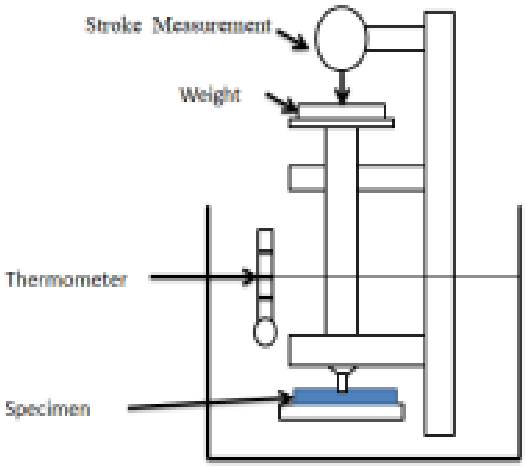

Fig. 17. Schematic Diagram of Vicat Softening Temperature

Fig. 18a. Vicat Softening Temperature specimen of Pure PETG

Fig. 18b. Vicat Softening Temperature specimen of 10% CFPETG

Fig. 18c. Vicat Softening Temperature specimen of 20% CF-PETG

Fig.18d. Vicat Softening Temperature specimen of 30% CF-PETG

Fig. 18. Vicat Softening Temperature Specimens

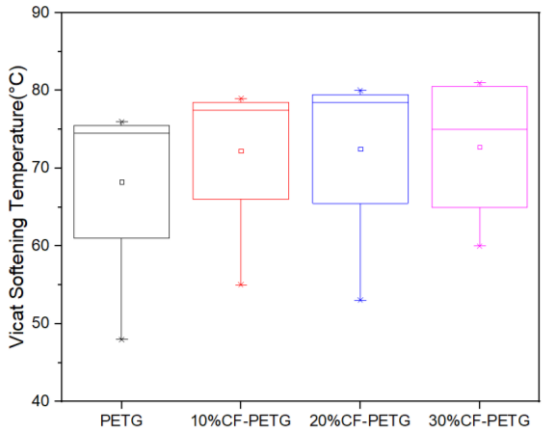

Fig. 19. Comparison of Vicat Softening Temperature of PETG

Table 6. Experimental results of the Flexural test

Material Name	Vicat Softening Temperature (°C)
PETG	74
10% CF-PETG	78
20% CF-PETG	79
30% CF-PETG	81

3.5. Heat Deflection Test

Five specimens were prepared for each composition of PETG, 10% CF-PETG, 20% CF-PETG, and 30% CF-PETG, as shown in Figure 20 and 21, following the ASTM standard D648 for the Heat Deflection test. The specimens were created using the FDM 3D printer, with a layer height of 0.1 mm and 100% infill density.

The purpose of the heat deflection test was to determine the temperature at which deformation occurs. Table 7 displays the heat deflection of the specimens based on the carbon percentage. Figures 22 depict a visual comparison of the values derived from the experimental data.

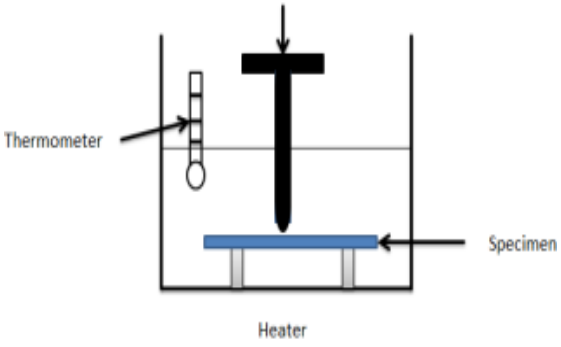

Fig. 20. Schematic Diagram of Heat Deflection Test

Fig. 21a. Heat Deflection Test specimen of Pure PETG

Fig. 21b. Heat Deflection Test specimen of 10% CFPETG

Fig. 21c. Heat Deflection Test specimen of 20% CF-PETG

Fig. 21d. Heat Deflection Test specimen of 30%CF-PETG

Fig. 21. Heat Deflection Test specimens

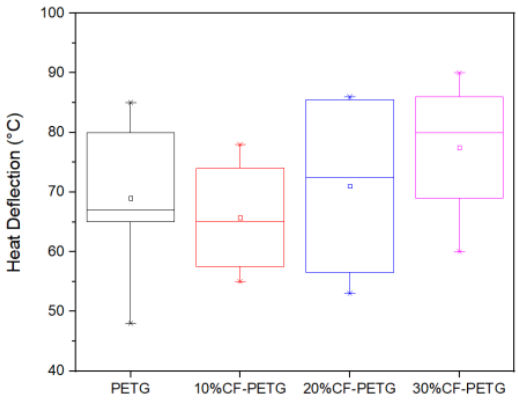

Fig. 22. Comparison of Heat Deflection Test D of PETG

Table 7. Experimental results of Heat Deflection Test

Material Name	Heat Deflection Test (°C)
PETG	67
10% CF-PETG	70
20% CF-PETG	86
30% CF-PETG	90

4. Finite Element Analysis

4.1. Compression Test for PETG

The PETG component, conforming to the ASTM D695 standard, was analysed using the Ansys Workbench 23.0® software. Initially, a 2D diagram with zero thickness, following the ASTM standard, was created using Creo Parametric 9.0®. The material was assigned first after that part was imported to the ANSYS ACP® and then created as per the thickness of the component, the orientation set for the solid model was generated, Including the supports of the two components of the solid model one was placed fixed at the bottom of the solid component and another one was kept above the specimen for the remote displacement, the above two supports was also designed by using the creo parametric® software, then it was imported to the ansys workbench® for assign the degree of freedom for the analysis, the pre and post

analysis was performed and the analysis of von misses stress, total deformation of the material was mentioned in the following figure 23 and 24 and table 8.

A linear elastic material model was used for PETG and CF-PETG composites in finite element simulations. The major focus on elastic stiffness, the need for simplified comparisons with experimental flexural tests, and the lack of significant plasticity data for CF-PETG prevented this work from considering plasticity. Modelling PETG's plastic deformation requires stress-strain data beyond the yield point and advanced calibration methods, which this study did not have. The addition of nonlinear material behaviour would have increased computing complexity. Future studies will focus on elasto-plastic modelling using experimentally calibrated plasticity parameters to improve simulation prediction.

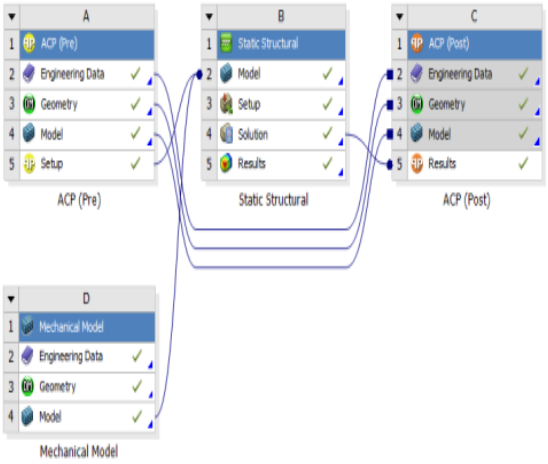

Fig. 23. Ansys ACP setup for Compression Test

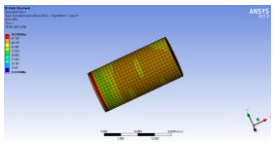

Fig. 24a. Equivalent Stress (Pure PETG)

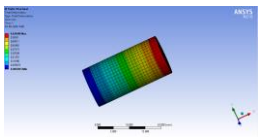

Fig. 24b. Total Deformation (Pure PETG)

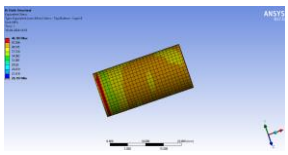

Fig. 24c. Equivalent Stress (10% CF-PETG)

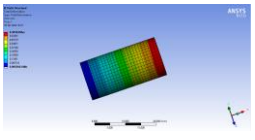

Fig. 24d. Total Deformation (10% CF-PETG)

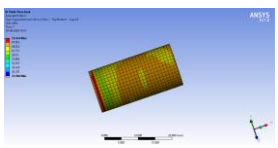

Fig. 24e. Equivalent Stress (20% CF-PETG)

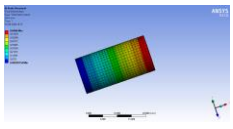

Fig. 24f. Total Deformation (20% CF-PETG)

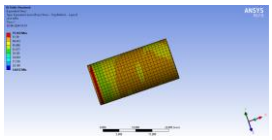

Fig. 24g. Equivalent Stress (30% CF-PETG)

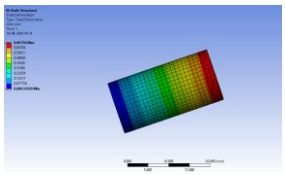

Fig. 24h. Total Deformation (30% CF-PETG)

Fig. 24. Compression Test - Numerical Analysis results

Table 8. Compression Test Results

ASTM standard	Material	Yield strength (MPa)	Von mises Stress (MPa)	Total deformation (mm)
ASTM D695	PETG	49	50.258	0.63649
	10% CF - PETG	48	46.187	0.58594
	20% CF - PETG	50	51.1074	0.6466
	30% CF - PETG	54.987	55.162	0.69716

4.2. Flexural Test for PETG

Using Ansys Workbench 23.0®, the PETG component was analysed in accordance with ASTM D790 standards. First, using Creo Parametric 9.0®, a 2D diagram with zero thickness was drawn in accordance with the ASTM standard. The part was imported into ANSYS ACP®, the material was assigned first, and the solid model's orientation was generated based on the component's thickness. The three solid model components' supports were designed using the Creo parametric® software. Two of the supports were positioned at the bottom of the solid component, and the third was kept above the specimen for remote displacement. The degree of freedom for the analysis was then assigned, and also performed von Mises stress analysis, and total deformation of the material, as shown in the following figures 25 and 26, Table 9.

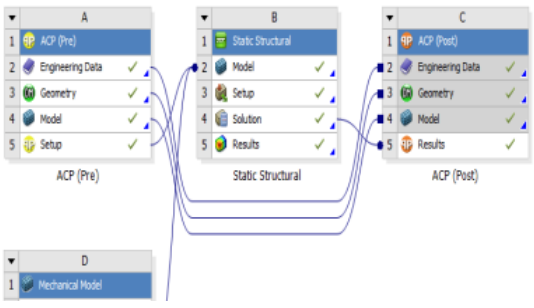

Fig. 25. Ansys ACP setup for Flexural Test

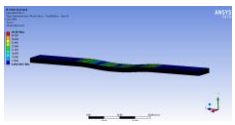

Fig. 26a. Equivalent Stress (Pure PETG)

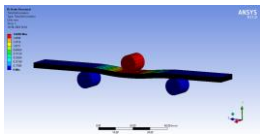

Fig. 26b. Total Deformation (Pure PETG)

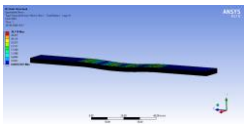

Fig. 26c. Equivalent Stress (10% CF-PETG)

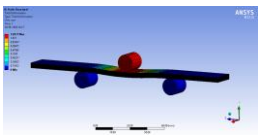

Fig. 26d. Total Deformation (10% CF-PETG)

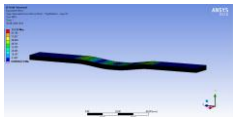

Fig. 26e. Equivalent Stress (20% CF-PETG)

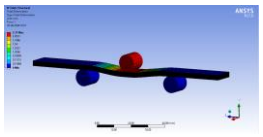

Fig. 26f. Total Deformation (20% CF-PETG)

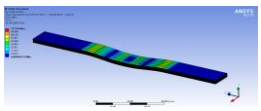

Fig. 26g. Equivalent Stress (30% CF-PETG)

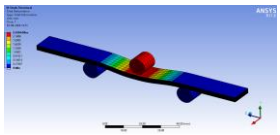

Fig. 26h. Total Deformation (30% CF-PETG)

Fig. 26. Flexural Test - Numerical Analysis results

Table 9. Flexural Test Results

ASTM standard	Material	Yield strength (MPa)	Von mises stress (MPa)	Total deformation (mm)
ASTM D790	PETG	50	49.492	1.6096
	10% CF - PETG	39	38.719	1.2071
	20% CF - PETG	76	73.333	2.31
	30% CF – PETG	77	77.519	2.4306

5. Results and Discussions

The results of the experimental tests (Compression and Flexural) were compared to the numerical analysis, and the differences in the values are presented in Tables 10 and 11.

The smallest percentage deviation was obtained by comparing results. There is a direct relationship between the amount of carbon fibre added to the PETG material and the results of the Vicat softening temperature, heat deflection, and hardness tests. This conclusion is based on the empirical results obtained for PETG, 10% CF-PETG, 20% CF-PETG, and 30% CF-PETG. Incorporating carbon fibre into the PETG material enhances its mechanical properties. The graph depicts the range of results obtained from the mechanical test performed on PETG, 10% CF-PETG, 20% CF-PETG, and 30% CF-PETG.

Table 10. Comparison of Experimental Results with Numerical Simulation for Compression Test

Material	Experimental Yield Strength (MPa)	Simulation Yield Strength (MPa)	Error %
PETG	53	49	7.5
10%CF-PETG	49	48	2.04
20%CF-PETG	54	50	7.4
30%CF-PETG	58	54.987	5.19

Table 11. Comparison of Experimental Results with Numerical Simulation for Flexural Testing

Material	Experimental yield strength (MPa)	Simulation yield strength (MPa)	Error %
PETG	54	50	7.4
10%CF-PETG	43	39	9.3
20%CF-PETG	77	76	1.2
30%CF-PETG	80	77	3.75

6. Conclusions

- The experimental study analysed the mechanical properties of composite materials composed of Carbon fibre reinforced with PETG polymer. The parameters investigated included Compression Strength, Flexural Strength, Shore Hardness (D), Vicat Softening Temperature, and Heat Deflection Test,

and the stress values were obtained from these experiments.

- In the Experimental test comparison, 30% CF-PETG obtained the highest values, depending on the various process parameters.
  - Compression value - 58 MPa,
  - Flexural value - 80MPa,
  - Shore Hardness (D) value - 77,
  - Vicat Softening Temperature - 81°C
  - Heat Deflection Test - 90°C.
- The carbon fiber-reinforced polymer was subjected to compression and flexural tests, which were simulated using ANSYS Workbench23.0®. The investigation specifically examined the factors of stress and overall deformation, and the minimum error value of < 10% validated the experimental values.
- The addition of carbon fibre to the PETG material significantly enhanced its mechanical properties.
- This study found that PETG and CF-PETG composites have equal strain at break values, contrast to the assumption that fibre reinforcement affects flexibility. Effective stress transfer from the matrix to the fibres, optimised printing conditions, and fiber-matrix interaction prevent early failure. Fibre length, orientation, and dispersion also keep PETG ductile.
- Load transfer efficiency, interfacial adhesion, fibre orientation, and defect formation affect CF-PETG composite mechanical properties. Due to stress distribution, fibre improves tensile and flexural characteristics, but too much fibre can cause agglomeration, porosity, and premature failure. Almost identical strain upon break shows balanced fiber-matrix interaction, preventing brittleness. Printing voids and anisotropic fibre orientation cause compressive and flexural strength nonlinearity. Further research will use microscopic failure analysis and numerical modelling to determine microstructural causes of these patterns.

Acknowledgements

The authors would like to express their sincere thanks to Ramco Institute of Technology, Rajapalayam, P.S.R. Engineering College, Sivakasi, for providing the necessary facilities and continuous support and encouragement to carry out this research work.

Funding Statement

This research did not receive any specific grant from funding agencies in the public, commercial, or not-for-profit sectors.

Conflicts of Interest

The author declares that there is no conflict of interest regarding the publication of this article.

References

[1] Alhat, S. M. and Yadav, M. H., 2020. Mechanical and electrical behavior of polyethylene terephthalate glycol (PETG) reinforced with multiwall carbon nanotubes (MWCNT) by using fused deposition modeling 3D printing *Int. Res. J. Eng. Technol.*, *7*(5), pp.1405-1413. Available: www.irjet.net

[2] Vallejo, J., García-Plaza, E., Núñez, P. J., Chacón, J. M., Caminero, M. A. and Romero, A., 2023. Machinability analysis of carbon fibre reinforced PET-Glycol composites processed by additive manufacturing. *Composites Part A: Applied Science and Manufacturing*, *172*, p.107561. doi: 10.1016/j.compositesa.2023.107561.

[3] Srinidhi, M. S., Soundararajan, R., Satishkumar, K. S. and Suresh, S., 2021. Enhancing the FDM infill pattern outcomes of mechanical behavior for as-built and annealed PETG and CFPETG composites parts. *Materials Today: Proceedings,* 45, pp. 7208–7212, doi: 10.1016/j.matpr.2021.02.417.

[4] Alarifi, I. M., 2023. Mechanical properties and numerical simulation of FDM 3D printed PETG/carbon composite unit structures. *J. Mater. Res. Technol.*, 23, pp. 656–669. doi:10.1016/j.jmrt.2023.01.043.

[5] Khan, I., et al., 2023. Parametric investigation and optimisation of mechanical properties of thick tri-material based composite of PLA–PETG–ABS 3D-printed using fused filament fabrication.

Compos. Part C: Open Access, 12, 100392. doi:10.1016/j.jcomc.2023.100392.

[6] Alarifi, I. M., 2023. PETG/carbon fiber composites with different structures produced by 3D printing. *Polym. Test.*, 120, p.107949. doi:10.1016/j.polymertesting.2023.107949.

[7] Li, Y. and Sharif-Khodaei, Z., 2024. A novel damage detection method for carbon fibre reinforced polymer structures based on distributed strain measurements with fibre optical sensor. *Mech. Syst. Signal Process.*, 208, p.110954. doi:10.1016/j.ymssp.2023.110954.

[8] Wan, X., et al., 2024. Elevating mechanical and biotribological properties of carbon fiber composites by constructing graphene–silicon nitride nanowires interlocking interfacial enhancement. *J. Mater.*, 10(5), pp. 1080–1090. doi:10.1016/j.jmat.2023.11.009.

[9] Popa, C. F., Marghitas, M. P., Galatanu, S. V. and Marsavina, L., 2022. Influence of thickness on the IZOD impact strength of FDM printed specimens from PLA and PETG. *Procedia Struct. Integr.,* 41, pp. 557–563. doi:10.1016/j.prostr.2022.05.064.

[10] Kumar, M. A., Khan, M. S. and Mishra, S. B., 2020. Effect of machine parameters on strength and hardness of FDM printed carbon fiber reinforced PETG thermoplastics. *Mater. Today: Proc.,* 27, pp. 975–983. doi:10.1016/j.matpr.2020.01.291.

[11] García, E., Núñez, P. J., Caminero, M. A., Chacón, J. M. and Kamarthi, S., 2022. Effects of carbon fibre reinforcement on the geometric properties of PETG-based filament using FFF additive manufacturing. *Compos. Part B: Eng.*, 235, p.109766. doi:10.1016/j.compositesb.2022.109766.

[12] Yan, C., et al., 2024. PETG: Applications in modern medicine. *Eng. Regen.,* 5(1), pp. 45–55. doi:10.1016/j.engreg.2023.11.001.

[13] Pheysey, J., De Cola, F., Pellegrino, A. and Martinez-Hergueta, F., 2024. Strain rate and temperature dependence of short/unidirectional carbon fibre PEEK hybrid composites. *Compos. Part B: Eng.,* 268, 111080. doi:10.1016/j.compositesb.2023.111080.

[14] Valvez, S., Silva, A. P. and Reis, P. N. B., 2022. Compressive behaviour of 3D-printed PETG composites. *Aerospace*, 9(3), 124. doi:10.3390/aerospace9030124.

[15] Soleyman, E., et al., 2022. Assessment of controllable shape transformation, potential applications, and tensile shape memory properties of 3D printed PETG. *J. Mater. Res. Technol.,* 18, pp. 4201–4215. doi:10.1016/j.jmrt.2022.04.076.

[16] Uzzell, J. P. N., Pickard, L. R., Hamerton, I. and Ivanov, D. S., 2024. Novel cellular coil design for improved temperature uniformity in inductive heating of carbon fibre composites. *Mater. Des.,* 237, 112551. doi:10.1016/j.matdes.2023.112551.

[17] Yan, J., Demirci, E. and Gleadall, A., 2023. Are classical fibre composite models appropriate for material extrusion additive manufacturing? A thorough evaluation of analytical models. *Addit. Manuf.*, 62, 103371. doi:10.1016/j.addma.2022.103371.

[18] Patel, K. S., Shah, D. B., Joshi, S. J., Aldawood, F. K. and Kchaou, M., 2024. Effect of process parameters on the mechanical performance of FDM printed carbon fiber reinforced PETG. *J. Mater. Res. Technol.,* 30, pp. 8006–8018. doi:10.1016/j.jmrt.2024.05.184.

[19] Qu, P., et al., 2024. Additive manufacturing of hybrid continuous carbon/basalt fiber reinforced composites based on bi-matrix co-extrusion. *J. Mater. Res. Technol.,* 30, pp. 8683–8704. doi:10.1016/j.jmrt.2024.05.241.

[20] Patel, K. S., Shah, D. B., Joshi, S. J. and Patel, K. M., 2023. Developments in 3D printing of carbon fiber reinforced polymer containing recycled plastic waste: A review. *Clean. Mater.,* 9, 100207. doi:10.1016/j.clema.2023.100207.

[21] Prabhakaran, R., Pitchipoo, P., Rajakarunakaran, S. and Venkatesh, R., 2024. Experimental investigation and optimization of process parameters on digital light processing (DLP) 3D printing process based on Taguchi-grey relational analysis. *Proceedings of the Institution of Mechanical Engineers, Part E: Journal of Process Mechanical Engineering,* 238(4), pp. 1884–1893. doi:10.1177/09544089241236267.

[22] Wang, W., Lin, Y., Hu, Y., Yang, L., Lin, D., Ma, J., Zhou, L., Liu, B., Cai, X., Yan, C. and Shi, Y., 2025. The effect of fatigue loading on the mechanical properties of additively manufactured continuous carbon fiber-reinforced composites. *Compos. Commun.,* 53, p.102231. doi:10.1016/j.coco.2024.102231.

[23] Venkatesh, R., Kathiravan, S., Prabhakaran, R., Ramar, M., Britto, J. J. J. and Rajakarunakaran, S., 2022. Experimental investigation on machinability of additive manufactured PLA and PETG polymers under dry turning process. *In: Recent Advances in Materials Technologies, Lecture Notes in Mechanical Engineering*, pp. 553–561. doi:10.1007/978-981-19-3895-5_45.

[24] Prabhakaran, R., Britto, J. J. J., Venkatesh, R., Mukesh, G. and Mohamedabrar, I., 2022. Experimental investigation and identifying the suitable process parameters for additively manufactured PETG material by fused deposition modeling. *In: Recent Advances in Materials Technologies, Lecture Notes in Mechanical Engineering*, pp. 541–552. doi:10.1007/978-981-19-3895-5_44.

[25] Venkatesh, R., Prabhakaran, R., Jerold John Britto, J., Amudhan, K. and Karan Kumar, G., 2022. Evaluation of Hardness, Surface Roughness, and Impact Strength of Additive Manufactured Ultraviolet Resin-Based Polymer. *In Recent Advances in Materials Technologies: Select Proceedings of ICEMT 2021,* (pp. 267-274). Singapore: Springer Nature Singapore. doi:10.1007/978-981-19-3895-5_21.